LNGS - 94/115
December 1994

MACRO/PUB 94/2

Search for Magnetic Monopoles with the MACRO Track-etch Detector

S. Ahlen[3], M. Ambrosio[12], R. Antolini[7], G. Auriemma[14,a], R. Baker[11], A. Baldini[13], G.C. Barbarino[12], B.C. Barish[4], G. Battistoni[6,19*], R. Bellotti[1], C. Bemporad[13], P. Bernardini[10], H. Bilokon[6], V. Bisi[16], C. Bloise[6], C. Bower[8], S. Bussino[14], F. Cafagna[1], M. Calicchio[1], D. Campana[12], M. Carboni[6], S. Cecchini[2,b], F. Cei[13], V. Chiarella[6], A. Corona[14], S. Coutu[11], G. De Cataldo[1], H. Dekhissi[2,c], C. De Marzo[1], I. De Mitri[9], M. De Vincenzi[14,d], A. Di Credico[7], E. Diehl[11], O. Erriquez[1], C. Favuzzi[1], C. Forti[6], P. Fusco[1], G. Giacomelli[2], G. Giannini[13,e], N. Giglietto[1], M. Goretti[14], M. Grassi[13], P. Green[15,18*], A. Grillo[6], F. Guarino[12], P. Guarnaccia[1], C. Gustavino[7], A. Habig[8], K. Hanson[11], R. Heinz[8], J.T. Hong[3], E. Iarocci[6,f], E. Katsavounidis[4], E. Kearns[3], S. Kyriazopoulou[4], E. Lamanna[14], C. Lane[5], D. S. Levin[11], P. Lipari[14], G. Liu[4], R. Liu[4], M.J. Longo[11], Y. Lu[15], G. Ludlam[3], G. Mancarella[10], G. Mandrioli[2], A. Margiotta-Neri[2], A. Marin[3], A. Marini[6], D. Martello[10,17*], A. Marzari Chiesa[16], M.N. Mazziotta[1], D.G. Michael[4], S. Mikheyev[7,g], L. Miller[8], M. Mittelbrun[5], P. Monacelli[9], T. Montaruli[1], M. Monteno[16], S. Mufson[8], J. Musser[8], D. Nicoló[13], R. Nolty[4], C. Okada[3], G. Osteria[12], O. Palamara[10], S. Parlati[4,7*], V. Patera[6,f], L. Patrizii[2], B. Pavesi[2], R. Pazzi[13], C.W. Peck[4], J. Petrakis[8,17*], S. Petrera[10], N.D. Pignatano[4], P. Pistilli[10], V. Popa[2,h], G. Pugliese[14], A. Rainó[1], J. Reynoldson[7], F. Ronga[6], A. Sanzgiri[15], F. Sartogo[14], C. Satriano[14,a], L. Satta[6,f], E. Scapparone[2], K. Scholberg[4], A. Sciubba[6,f], P. Serra Lugaresi[2], M. Severi[14], M. Sitta[16], P. F. Spada[2], P. Spinelli[1], M. Spinetti[6], M. Spurio[2], R. Steinberg[5], J.L. Stone[3], L.R. Sulak[3], A. Surdo[10], G. Tarlé[11], V. Togo[2], V. Valente[6], E. Vilela[2,i], C.W. Walter[4], R. Webb[15] and W. Worstell[3].

(MACRO Collaboration)

1. Dipartimento di Fisica dell'Università di Bari and INFN, Bari, 70126, Italy
2. Dipartimento di Fisica dell'Università di Bologna and INFN, Bologna, 40126, Italy
3. Physics Department, Boston University, Boston, MA 02215, USA
4. California Institute of Technology, Pasadena, CA 91125, USA
5. Department of Physics, Drexel University, Philadelphia, PA 19104, USA
6. Laboratori Nazionali di Frascati dell'INFN, Frascati (Roma), 00044, Italy
7. Laboratori Nazionali del Gran Sasso dell'INFN, Assergi (L'Aquila), 67010, Italy
8. Depts. of Physics and of Astronomy, Indiana University, Bloomington, IN 47405, USA
9. Dipartimento di Fisica dell'Università dell'Aquila and INFN, L'Aquila, 67100, Italy

10. Dipartimento di Fisica dell'Università di Lecce and INFN, Lecce, 73100, Italy
11. Department of Physics, University of Michigan, Ann Arbor, MI 48109, USA
12. Dipartimento di Fisica dell'Università di Napoli and INFN, Napoli, 80125, Italy
13. Dipartimento di Fisica dell'Università di Pisa and INFN, Pisa, 56010, Italy
14. Dipartimento di Fisica dell'Università di Roma and INFN, Roma, 00185, Italy
15. Physics Department, Texas A&M University, College Station, TX 77843, USA
16. Dipartimento di Fisica Sperimentale dell'Università di Torino and INFN, Torino, 10125, Italy
17. Bartol Research Institute, University of Delaware, Newark, DE 19716, USA
18. Sandia National Laboratory, Albuquerque, NM 87185, USA
19. INFN Sezione di Milano, 20133, Italy
⋆ Current address
a Also Università della Basilicata, Potenza, 85100, Italy
b Also Istituto TESRE/CNR, Bologna, Italy
c Also at Faculty of Science, University Mohamed I, Oujda, Morocco
d Also at Università di Camerino, Camerino, Italy
e Also Università di Trieste and INFN, Trieste, 34100, Italy
f Also Dipartimento di Energetica, Università di Roma, Roma, 00185, Italy
g Also at Institute for Nuclear Research, Russian Academy of Science, Moscow, Russia
h Now at Institute of Gravity and Space Sciences, R-76900, Bucharest, Romania
i Now at Inst. de Pesquisas Energéticas e Nucl., Pinheiros 05422-970 São Paulo, Brazil

Abstract

In this note we discuss the experimental techniques, the calibrations and the preliminary limits obtained on the search for magnetic monopoles using the MACRO track-etch subdetector as a stand alone detector. The flux upper limits are at the level of $1.6 \times 10^{-14} cm^{-2} s^{-1} sr^{-1}$ for $\beta > 6 \times 10^{-2}$ and $2.4 \times 10^{-14} cm^{-2} s^{-1} sr^{-1}$ at $\beta \approx 10^{-4}$.

1 Introduction

The MACRO experiment has a modular structure with three types of detectors: streamer tubes, liquid scintillators and nuclear track detectors. The lower structure has ten horizontal planes of limited streamer tubes, two horizontal planes of scintillators, one horizontal plane of track-ecth detectors and seven horizontal layers of passive rock absorbers. The upper part has four layers of streamer tubes and one layer of scintillators. The sides of MACRO are covered with 6 layers of streamer tubes and 1 layer of scintillators. Nuclear track detectors are positioned also on the east and north vertical walls. The complete MACRO structure has overall dimensions of $12\times77\times9$ m^3. The apparatus is documented in detail elsewhere [1].

In this note we discuss the techniques, the calibrations and the preliminary results of the magnetic monopole search using the MACRO track-etch detector [2-5] as a stand alone detector. (A monopole search using the MACRO liquid scintillators is reported in [6]). In particular we focus our attention on the CR39 fabrication, on the tests and etching conditions, on the methods of searching for candidate events and on the determination of the geometrical and detection efficiencies. An updated estimate of the upper limits on the monopole flux established by the MACRO nuclear track detector is also presented. Note that every time we removed "wagons" of nuclear track detectors, we substituted them with new ones, containing new CR39 of improved sensitivity (L6 type). It may be worth recalling that the MACRO track-etch detector is also used in a "triggered" mode in conjunction with the streamer tube and scintillator systems.

2 The MACRO track-etch detector

The main part of the track-etch detector is located horizontally in the middle of the lower modules of MACRO, just above the 5th layer of streamer tubes. Each of the six lower supermodules is equipped with 48 "trains" consisting of 47 "wagons" (stacks) of nuclear track detectors (a total of 13536 horizontal "wagons"). Each "wagon" contains three layers of CR39, each about 1.4 mm thick, three layers of lexan, each 0.25 mm thick, and a 1 mm

thick aluminium absorber. Each stack is placed in an aluminized mylar bag filled with dry air [2]. The surface of each stack is 24.5 × 24.5 cm^2=600.25 cm^2 = 0.060 m^2. The effective surface of the horizontal CR39 is 812.5 m^2. The track-etch detector has also been installed on the east wall and on the lower part of the north wall. On the north vertical surface there are 816 wagons of nuclear track detectors of 24 × 24 cm^2 area, corresponding to 47 m^2. On the east wall, lower and upper, there are 7008 wagons, corresponding to 403.7 m^2. The total nuclear track detector surface is thus 1263.2 m^2.

3 The CR39 nuclear track detector

Although MACRO's track-etch detector consists of two types of nuclear track detectors, CR39 and Lexan, most of the work concerns the development and processing of the CR39. Lexan has a much higher threshold (REL$\approx$ 3 $GeVcm^2/g$) compared to that of CR39, making it primarily sensitive to relativistic monopoles. Lexan has not been used until now for monopole searches in MACRO.

The CR39 used in MACRO is produced by the INTERCAST Company of Parma, Italy. The standard CR39, that is used mainly for sun glasses, was improved in order to achieve a lower detection threshold, a higher sensitivity in a large range of energy losses, a high quality of the post- etched surface after prolonged etching, stability of the sensitivity of the polymer over long periods of time (at least several years) and uniformity of sensitivity for mass produced sheets. In order to achieve these goals, a specific scientific line of production was designed and implemented [5]. Two types of CR39 have been developed, containing different additives and using different catalyzers and curing cycles: the EN3 type, that was used in the first supermodule of MACRO, and the L6 type, that was installed in all the other supermodules and on the vertical walls. The EN3 type CR39 was produced using the CHPC catalyzer, the DOP additive and a curing cycle with a maximum temperature of 80°C. The L6 version is produced using the IPP catalyzer, the Naugard N445 antioxidant additive and a curing cycle with a maximum temperature of 95°C.

Three types of etching conditions were used: (i) "normal" etching for most standard work: in 6N NaOH solution at 70°C; (ii) "fast" etching, 8N NaOH

at 80°C, for fast searches for monopoles in the top CR39 layer; (iii) "slow" etching, 6N, 40°C, for the detection of very slow ions. The bulk etching rates (v_B) measured in 6N solutions of NaOH at 70°C are $v_B = (1.25 \pm 0.02)\mu$m/h for the EN3 polymer and $(1.16 \pm 0.02)\mu$m/h for the L6 type of CR39 [5]. The corresponding rates in 8N solutions at 80°C are $(5.74 \pm 0.57)\mu$m/h for EN3 and $(4.12 \pm 0.21)\mu$m/h for L6; at 40°C in 6N solutions we have $v_B = (0.100 \pm 0.002)\mu$m/h for the L6 type. Presently, the CR39 production for MACRO is restricted to the improved L6 CR39 type only.

4 The calibration of CR39

Previous tests made on the two types of CR39 plastic detectors, the EN3 and the L6 ones [4], indicated that the last one is the most suitable, having a lower detection threshold (26 $MeVcm^2/g$ for L6 compared with 53 $MeVcm^2/g$ for EN3 [4]) and a better surface quality. Thus all of MACRO, with the exception of the first supermodule, is equipped with the L6 type CR39. A summary of the calibration exposures made so far is presented in Table 1.

4.1 Calibrations with relativistic ions

Both types of CR39 were tested and calibrated with relativistic heavy ions: (i) with oxygen nuclei of 16 A GeV at Brookhaven (1988), (ii) with neon nuclei of 585 A MeV at Berkeley (1990), with (iii) silicon nuclei of 14.5 A GeV at Brookhaven (1990), (iv) with sulphur nuclei of 200 A GeV at CERN (1990) and (v) with gold nuclei of 11.3 A GeV at Brookhaven (1992) [4-5,7-10]. For these purposes, stacks of few sheets (7×13) cm^2 in size of CR39 located before and after a copper or aluminium target were exposed to a total flux of approximately 1500 $ions/cm^2$. Both the primary ions and their fragments have been used for the calibrations.

For each of the incoming particle and its fragments we calculated the restricted energy loss (REL) as given by the formula:

$$\left(\frac{dE}{dx}\right)_{E<E_0=200eV} = 4\pi N_a r_e^2 m_e c^2 (\frac{z}{\beta})^2 \frac{Z}{A} \left[ln \left(\frac{\sqrt{2m_e c^2 \beta^2 \gamma^2 E_0}}{I} \right) - \frac{\beta^2}{2} - \frac{\delta}{2} \right] \quad (1)$$

where z/β refers to the incoming particle (ion fragments), Z/A to the target and $N_a r_e^2 m_e c^2 = 0.307 MeV cm^2 g^{-1}$; for CR39: Z/A = 0.533; the mean ionization potential is I=70 eV. The density correction δ was calculated according to ref.[11].

The reduced etching ratio $p = v_T/v_B$ -that traditionally has been the signal measured from a nuclear track detector- was calculated based on the measurement of the surface areas of the etch-pits and the previous knowledge of the bulk etching velocity v_B. Surface areas were measured with an ELBEK automatic image analyzer system [12].

For the two types of CR39, EN3 and L6, we plot in Fig. 1 the measured signal p versus the REL for the gold ions/fragments to which the CR39 was exposed. The L6 type has a threshold of 26 MeV cm^2/g (corresponding to $z/\beta \sim 5$) , clearly much lower than the one obtained for EN3 (53 MeV cm^2/g, corresponding to $z/\beta \sim 7.5$).

Further studies of CR39's stability over long periods of time have been performed. In May 1992 we have exposed pieces of CR39 manufactured at different times (Feb '90, Jan '91 and Jan '92) to 11.3 A GeV gold (Au^{79+}) ions and compared the measured signal for the various fragments. As shown in Fig. 2, within our experimental uncertainties (of the order of 10%) the three calibration curves obtained in this way agree quite well.

Finally, using relativistic ions and their fragments, we examined the response of our detector under different etching conditions. Using sulphur (S^{16+}) ions of 200 A GeV we etched the exposed CR39 under two different etching conditions: 8N NaOH at 80°C and 6N NaOH at 70°C. Samples of CR39 exposed to gold (Au^{79+}) ions of 11.3 A GeV were etched in 6N NaOH at 40°C. The detector's response under the different etching conditions is shown in Fig. 3. The data show that while the detection threshold is not significantly altered, the sensitivity of the CR39 increases as the etching becomes stronger. Nevertheless, we must stress that the surface and the track properties are negatively affected by stronger etching.

4.2 Calibrations with slow ions ($\beta < 10^{-2}$)

A calibration with slow ions (silicon, beryllium, protons and deuterons of energies between 50 and 400 keV, corresponding to $3.9 \times 10^{-3} < \beta < 2.07 \times 10^{-2}$) has now been completed [10]. The calibration was performed to test the response of CR39 to particles in the mentioned velocity range and to see if only part or all of the nuclear energy loss is effective to the latent track formation (see [10,13]). Fig. 4 shows for the L6 type of CR39 the calibration curves obtained with completely ionized relativistic ions, 100-400 keV beryllium ions, 200-400 keV silicon ions, with 50-200 keV hydrogen and deuterons and 6-10 MeV helium ions, He^{2+}. The charge of the beryllium and silicon ions was $+1e$ at energies less than 200 keV and $+2e$ at greater energies. The etching was performed in 6N NaOH solutions at 40°C, as already stated; in this condition the bulk etching rate was 0.1 μm/h. The parameters of the etched pits (which are (0.2-0.8)μm deep) were measured making plastic replicas and measuring them with a Scanning Electron Microscope (SEM). We took great care to avoid bending and stretching the replica cones and to make the proper observations with the SEM.

As shown in Fig. 4, a single curve -within our experimental errors inclusive of systematic uncertainties for the low velocity data- of p versus REL can describe our detector's response for both fast and slow ($\beta < 0.01$) ions when the total energy loss of the slow ions is taken into account; this is consistent with the predictions of the REL model for the CR39 response [10].

Snowden-Ifft and Price [13] studied the response of CR39 (with DOP additive), manufactured by American Acrylics (Wilmington, Delaware), to low velocity ($3 \times 10^{-3} < \beta < 10^{-2}$) ions. They concluded that their CR39's response versus REL at high velocities does not agree with the one obtained at low velocities. Furthermore they state that the nuclear stopping power is only 20% as effective as the electronic stopping power as far as the latent track formation is concerned. For our more sensitive CR39 (without DOP) we find that a single curve describes relativistic and low velocity ion data and that the data are consistent with $\simeq$ 100% contribution of the nuclear energy loss (with a lower limit of $\approx$ 80%).

5 The response of CR39 to monopoles

We computed the restricted energy loss (REL) as a function of the monopole velocity in CR39 for bare $g = g_D$ and $g = 3g_D$ monopoles as well as for monopoles with a proton or an aluminium nucleus attached (Fig. 5). The curves were computed from [14,15] for bare poles (M) and for (M+Al), from [15] for (M+p). The horizontal dotted lines represent the detection thresholds for the L6 and the EN3 varieties of CR39 [4]. For poles with $g = g_D$ the EN3 type CR39 should be sensitive for velocities in the range 3×10^{-5} c - 2.6×10^{-4} c and for velocities higher than 2×10^{-3} c. For the L6 type the β ranges are slightly larger, $(2 \div 3) \times 10^{-5} < \beta < 3.4 \times 10^{-4}$ and $\beta > 1.2 \times 10^{-3}$. If monopoles would carry an electric charge or have attached a nucleus the sensitivity would be adequate for poles of any speed higher than 3×10^{-5} c. Here we have assumed that monopoles with $m_M \geq 10^{17}$GeV and $g = g_D$ for $\beta = 3 \times 10^{-5}$ are not stopped by an Earth diameter, while monopoles with $g = 3g_D$ and (M+p) composites may be stopped by the Earth for $\beta < 5 \times 10^{-5}$. The analysis of this point is still in progress.

The response and the acceptance of the EN3 type CR39 for monopoles of different velocities and impinging with different angles were estimated using the formulae of [4]. The detection of magnetic monopoles is limited for poles with incidence angles smaller than a critical value δ_c (measured with respect to the normal) given by [16]

$$\delta_c = arccos(p^{-1}) \tag{2}$$

where p is the reduced etch rate. The acceptance $S\Omega$ for an isotropic flux is given by:

$$S\Omega = 2\pi S(1 - p^{-2}) \tag{3}$$

(at very low β the flux is not likely to be isotropic). We computed the acceptance of the CR39 sheets to an isotropic flux of magnetic monopoles for a combined surface of 1263 m^2 of CR39 of type EN3 and of type L6, Fig. 6. The lines correspond to $g = g_D$, $g = 3g_D$ monopoles and to M+p dyons, both for the L6 and EN3 types. We have assumed $m_M = 10^{17} GeV$; these monopoles are not stopped by the Earth even at $\beta =$ few 10^{-5} (thus these monopoles arrive from above and from below). Notice that for $\beta > 10^{-2}$ the acceptance of a 1000 m^2 array is about 6000 m^2 sr.

For our horizontal detector of S = 812.5 m^2, the acceptance is 4875 m^2sr. The approximate acceptance for the whole MACRO track-etch detector is about 7.1 $\times$ 10^3 m^2sr. Table 2 presents the geometric acceptance values obtained for both EN3 and L6 types of CR39, versus the monopole β, for a surface of 1000 m^2 of CR39 and for the actual detector. Values are given for the CR39 etched at both 70°C and 80°C.

6 The processing and scanning of the CR39 sheets

In the last two years, about half a "train" of CR39 of type EN3 (about 1.5 m^2) was extracted every few months from MACRO, without any electronic trigger. The exposure time of this CR39 was longer than 3 years (see Table 3).

After extraction, three fiducial holes of 2 mm diameter were drilled in each stack, by a precision drilling machine (the position of the holes is defined to within a 100 μm accuracy). Then the aluminium bags are opened, the plastic sheets are rotated and placed in new bags filled with dry air until chemical etching, which was done in Bologna.

The etching laboratory utilizes two tanks made of stainless steel and having inner dimensions of 40 cm x 52 cm x 40 cm, a volume of about 8.3 $\times$ 10^4 cm^3. Each tank can accommodate 24 CR39 25 cm x 25 cm sheets at once. One tank is reserved for etching and the other for pre-soaking and rinsing the sheets after etching. Three similar devices, of smaller dimensions, are now operational for the calibration sheets.

Two etching procedures are used: (i) A "strong" etching done in a (8.00 $\pm$ 0.02)N NaOH solution, at a temperature of (80.00 $\pm$ 0.02)°C, is applied to the first upper sheet of each wagon, and (ii) a "normal" etching is used for the second (and the third) CR39 layer in the case that a candidate hole is found in the upper sheet. The CR39 sheets are first pre-soaked and slowly heated to the etching temperature for 3-4 hours in pure water. Before chemical etching, all the required water is demineralised to yield an electric resistance of up to (18-20) $M\Omega$/cm and filtered for all organic impurities larger than 0.2 mm.

The strong etching is intended to reduce the thickness of the CR39 sheets

from about 1.4 mm to about 0.3 mm (it is difficult to handle thinner sheets). In order to avoid problems arising from the observed inhomogeneities of the material, the etching is performed in two steps. The first step lasts 65 h and leaves a thickness of about 0.7 mm. The CR39 plates are then rinsed in an acid solution obtained by combining 500 cm^3 of 99% CH_3COOH in 74 l of pure water. After about 20 hours of drying, the thickness of the sheets is measured at 64 fixed points distributed as an 8x8 matrix on the whole surface, using a semi-automatic device. The average known rate of etching and the thickness determined for each plate after the first 65 hours of etching is used to establish the duration of the second chemical etch, typically between 30 and 45 hours, in order to obtain a final thickness of the CR39 plates of about 0.3 mm. Before starting the second chemical etch, a fast scan is performed with a stereo microscope with low magnification (16x) and the position of every candidate is recorded.

The same procedure is repeated after the complete etching and all the possible candidates are checked. All of the etch rates information is stored for further reference. The comparison between the etching rates determined for the two etching periods is consistent with a constant etching rate of about $(5.74 \pm 0.57)\mu$m/h for the EN3 type of CR39 and with about $(4.12 \pm 0.21)\mu$m/h for the L6 type. The errors correspond to the standard deviation of the measured velocities and originate from the inhomogenities of the CR39 polymer. The strong etching procedure was calibrated with sulphur ions of 200 A GeV and it was found to yield (at both the first and second step of strong etching) clear, visible front-back coincident and equal pits, that eventually became holes at a residual thickness of 200 μm, achieved after 120 h of strong etching.

The careful observation of each sheet after the first and second strong etchings yields about one candidate event per m^2 of CR39. A more detailed analysis and a comparison of the front surface of the foil with its back surface reduces the number to 0.5 candidates per m^2. For these candidates we analysed the third CR39 layer using normal etching. Normal etching of CR39 is done in a (6.00 ± 0.02)N NaOH solution at a temperature of (70.00 ± 0.02)°C. The total etching time is determined after a first etching of 25 hours; after the second etching (of about 20 hours) the plates are examined using a precision microscope with high magnification (50x ob. and 16x oc.).

A candidate track must satisfy a two(three)-fold coincidence of the

positions and incident angles among the two (three) layers and should also give the same value of the restricted energy loss (REL). None such candidate was found.

7 Preliminary results

From 1991 we started the analysis of the track-etch detector as a "stand alone" detector. Up to now we have extracted 18.37 m^2 of CR39, mostly from the first supermodule; the present rate of etching is about half a "train" every few months. This rate is being increased as the etching and scanning capacity is increased. Table 3 summarizes the number of "wagons" etched and the evolution of the 90% confidence level upper limits of the monopole flux at $\beta \approx 1$ and at $\beta \approx 10^{-4}$ determined by the CR39 subdetector of MACRO. Since no candidates survive the complete analysis, the 90% C.L. upper limits are given by

$$\Phi < 2.3/(\Delta t S\Omega) \tag{4}$$

where Δt is the time exposure and $S\Omega$ is given by eq. (3). Since those limits are independent, they may be combined with the formula:

$$\Phi = 1/(1/\Phi_1 + 1/\Phi_2 + ... + 1/\Phi_n) \tag{5}$$

Fig. 7 illustrates our CR39 90% C.L. upper limits for an isotropic flux of monopoles versus β. For monopoles with $\beta > 6 \times 10^{-2}$ in CR39 the present limit is at the level of $1.6 \times 10^{-14} cm^{-2} s^{-1} sr^{-1}$; at $\beta \approx 10^{-4}$ the upper limit is at the level of $2.4 \times 10^{-14} cm^{-2} s^{-1} sr^{-1}$.

Acknowledgements

We gratefully acknowledge the technical support provided by the Gran Sasso National Laboratory and by our home Institutions. We thank the technical staff of Bologna and Torino sections of I.N.F.N. for the help in the installation and analysis of the CR39. We thank Dr. A. Fassó for his help in computing the acceptance of the track-ecth detector.

References

[1] MACRO collaboration; S. Ahlen et al. (First supermodule of the MACRO detector at Gran Sasso), Nucl. Instr. and Meth. in Phys. Res. A324 (1993) 337.

[2] MACRO collaboration; M. Calicchio et al. (The track-etch detector of the MACRO experiment) Nucl. Tracks Radiat. Meas. 15 (1988) 331.

[3] MACRO collaboration, R. Bellotti et al. (A search for magnetic monopoles with the MACRO detector at Gran Sasso), Proc. of the 21st Int. Cosmic Ray Conference, Adelaide (1990) vol. 10, 75.

[4] MACRO collaboration, R. Bellotti et al. (The track-etch detector for the MACRO experiment at the Gran Sasso laboratory), in: 21st Int. Cosmic Ray Conference, Adelaide (1990), vol.10, 252.

[5] MACRO collaboration; S. P. Ahlen et al. (Improvements in the CR39 polymer for the MACRO experiment at the Gran Sasso Laboratory) Nucl. Tracks Radiat. Meas. 19 (1991) 641.

[6] MACRO collaboration, S. Ahlen et al. (Search for slowly moving monopoles with the MACRO detector) Phys. Rev. Lett. 72 (1994) 608.

[7] MACRO Collaboration, R. Bellotti et al. (First results from the MACRO experiment at the Gran Sasso), Nucl Phys. B (Proc. Suppl.) 19 (1991) 128.

[8] S. Cecchini et al. (Calibration of the Intercast CR39) Nucl. Tracks Radiat. Meas. 22 (1993) 555.

[9] MACRO collaboration; S. Ahlen et al. (First supermodule of the MACRO detector at Gran Sasso), Nucl. Instr. and Meth. in Phys. Res. A324 (1993) 337.

[10] S. Cecchini et al. (Calibration with relativistic and low velocity ions of the CR39 nuclear track detector used in MACRO), to be submitted to Nucl. Instr. and Meth.

[11] W. R. Leo (Techniques for Nuclear and Particle Physics Experiments), Springer-Verlag, p. 26 (1987).

[12] A. Noll et al. (The Siegen automatic measuring system for nuclear track detectors: new developments), Nucl. Tracks Radiat. Meas., 15 (1988) 265.

[13] D. P. Snowden-Ifft and P. B. Price (The low velocity response of the solid state nuclear track detector CR-39), Phys. Lett. B 288 (1992) 250.

[14] S. Orito et al. (Search for Supermassive Relics with a 2000-m^2 Array of Plastic Track Detectors), Phys. Rev. Lett. 66 (1991) 1951.

[15] P. B. Price, (Limit on flux of supermassive monopoles and charged relic particles using plastic track detectors), Phys. Lett. B 140 (1984) 112.

[16] R. Fleischer, P. B. Price and R. M. Walker, Nuclear Tracks in Solids, University of California Press (1975) pp. 58-60.

Figure captions

Fig. 1 Reduced etch rate $p = v_T/v_B$ versus restricted energy loss (REL) for the nuclear track detectors CR39, of the L6 and EN3 types, with relativistic heavy ions (11.3 A GeV gold fragments). The standard etching (6N NaOH, 70°C) was used.

Fig. 2 Calibrations of the reduced etch rate p versus REL with relativistic Au ions on differently aged CR39. The irradiation was performed in May 1992, while the CR39 samples were produced in February 1990 (the stars), in January 1991 (the triangles) and in January 1992 (the circles). The standard etching (6N NaOH, 70°C) was used.

Fig. 3 Calibrations of the CR39 L6 type nuclear track-etch detectors with 200 A GeV sulphur ions corresponding to three different etching procedures: in 8N NaOH at 80°C (the circles), in 6N NaOH at 70°C (the squares) and with 11.3 A GeV Au ions and fragments (the triangles), in a 6N NaOH solution at 40°C.

Fig. 4 Calibrations of the CR39 L6 type nuclear track detector with relativistic and slow heavy ions. All etchings were performed in a 6N NaOH solution at 40°C.

Fig. 5 Restricted energy loss (REL) of bare $g = g_D$, $g = 3g_D$ monopoles and of (M + p) and (M + Al) systems versus their β in CR39. In the figure the thresholds for the EN3 and L6 types of CR39 are indicated.

Fig. 6 Acceptance $S\Omega$ for monopoles with $g = g_D$, $g = 3g_D$ and for M+p dyons, for the MACRO CR39 track-etch detector of types EN3 (dashed lines) and L6 (solid lines). (The approximate acceptance of the MACRO track-etch detector is $7.1 \times 10^3\ m^2sr$). The curves assume an isotropic flux of particles reaching the detector. For $\beta < 4 \times 10^{-5}$ there are uncertainties. Monopoles with $m_M \geq 10^{17}$ GeV will not be stopped by the Earth for $g = g_D$ and $\beta = 3 \times 10^{-5}$. Monopoles with $g = 3g_D$ and (M+p) composites may be stopped by an Earth diameter if they have a $\beta < 5 \times 10^{-5}$.

Fig. 7 The 90% confidence level upper limits for an isotropic flux of magnetic monopoles obtained with the CR39 subdetector of MACRO, for poles with $g = g_D$, $g = 3g_D$ and (M + p) composites, assuming $M = 10^{17}$ GeV. For $\beta < 4 \times 10^{-5}$ the same words of caution of Fig. 6 apply.

	Date	Ion	Energy	Site	Density (ion/cm^2)	Ref.
	Sept. 1988	O^{8+}	16 A GeV	AGS (BNL)	$(1 \div 2) \cdot 10^3$	[4]
FAST	Jan. 1990	Ne^{10+}	585 A MeV	BEVALAC (Berkeley)	$(1 \div 2)\ 10^3$	[5]
IONS	June 1990	Si^{14+}	14.5 A GeV	AGS (BNL)	$(1 \div 2)\ 10^3$	[8]
	July 1990	S^{16+}	200 A GeV	SPS (CERN)	$1.5 \cdot 10^3$	[4]
	May 1992	Au^{79+}	11.3 A GeV	AGS (BNL)	$1.5 \cdot 10^3$	This one, [10]
	May 1992 Dec. 1992	$Be^{1+,2+}$	100-400 keV	IICO (S. Clara, USA)	$\approx 10^8$	[10]
SLOW	May 1992 Dec. 1992	$Si^{1+,2+}$	200-400 keV	IICO (S. Clara, USA)	$\approx 10^8$	[10]
IONS	Dec. 1992	p,d	50-200 keV	IICO (S. Clara, USA)	$\approx 10^8$	[10]
	Feb. 1994	α	2-10 Mev	van de Graaff (Legnaro)	$\approx 10^3, 10^5$	[10]

Table 1. Summary of the CR39 calibration exposures.

β	SΩ for EN3 70 °C, 6N	SΩ for L6 70 °C, 6N	SΩ for L6 80 °C, 8N	MACRO ACCEPTANCE SΩ for L6 80 °C, 8N
$4.0\ 10^{-5}$	2489	3011	3269	4320
$5.0\ 10^{-5}$	3191	3664	3789	4500
$6.0\ 10^{-5}$	3570	4002	4058	4800
$8.0\ 10^{-5}$	3943	4331	4269	5040
$9.0\ 10^{-5}$	4039	4414	4195	4950
$1.0\ 10^{-4}$	4056	4429	4162	4920
$1.2\ 10^{-4}$	3925	4315	4270	5040
$1.4\ 10^{-4}$	3570	4002	4054	4790
$2.6\ 10^{-4}$	0	1400		
$3.2\ 10^{-4}$	0	0		
$1.2\ 10^{-3}$	0	0.1		
$1.9\ 10^{-3}$	0.1	1400		
$4.0\ 10^{-3}$	2489	3010	3268	4320
$7.0\ 10^{-3}$	3586	4016	4070	4810
$8.0\ 10^{-3}$	3841	4241	4245	5010
$1.0\ 10^{-2}$	4287	4630	4630	5430
$2.0\ 10^{-2}$	5226	5451	5451	6310
$3.0\ 10^{-2}$	5660	5826	5826	6690
$5.0\ 10^{-2}$	6054	6136	6136	6990
$6.0\ 10^{-2}$	6109	6175	6175	7020
$7.0\ 10^{-2}$	6152	6204	6204	7050
$8.0\ 10^{-2}$	6173	6218	6218	7070
$9.0\ 10^{-2}$	6182	6224	6224	7080
$1.0\ 10^{-1}$	6198	6235	6235	7090
$2.0\ 10^{-1}$	6240	6260	6260	7100
$3.0\ 10^{-1}$	6255	6268	6268	7110
$4.0\ 10^{-1}$	6265	6274	6274	7120
$5.0\ 10^{-1}$	6269	6276	6276	7120
$7.0\ 10^{-1}$	6274	6280	6280	7120
1	6274	6280	6280	7120

Table 2. Computed acceptances SΩ $[m^2 sr]$ of the CR39 track-etch detector (with S=1000 m^2) for $g = g_D$ monopoles and normal etching (6N, 70 °C) and strong etching (8N, 80 °C). In the last column the approximate total acceptance of the present MACRO track-etch detector is given.

Insertion date	Extraction date	Number of wagons	S $[m^2]$	CR39 type	Exposure time [yr]	90% C.L. Flux $[10^{-13}$ cm^{-2} s^{-1} $sr^{-1}]$ $(\beta = 1)$	Site	90% C.L. Flux combined $[10^{-15}$ cm^{-2} $s^{-1}sr^{-1}]$ $(\beta=1)$	90% C.L. Flux combined $[10^{-15}$ cm^{-2} $s^{-1}sr^{-1}]$ $(\beta = 10^{-4})$
9/11/88	4/4/90	6	0.36	EN3	1.40	23.0	BO		
10/11/88	4/4/90	2	0.12	EN3	1.40	69.2	BO		
7/9/88	25/6/90	2	0.12	EN3	1.80	53.8	BO		
6/9/88	5/7/90	6	0.36	EN3	1.83	17.6	BO		
8/9/88	5/7/90	3	0.18	EN3	1.82	35.4	BO		
12/9/88	5/7/90	3	0.18	EN3	1.81	35.6	BO		
10/10/88	5/7/90	4	0.24	EN3	1.73	27.9	BO		
6/9/88	5/2/91	20	1.20	EN3	2.42	4.00	BO		
6/9/88	7/2/91	4	0.24	EN3	2.42	20.0	BO		
6/9/88	9/4/91	20	1.20	EN3	2.59	3.74	BO		
5/7/90	9/4/91	1	0.06	L6	0.76	254	BO		
7/9/88	2/7/91	4	0.24	EN3	2.82	17.2	BO		
9/11/88	2/7/91	17	1.02	EN3	2.64	4.30	BO		
9/11/88	4/7/91	1	0.06	EN3	2.65	73.0	BO		
25/5/90	15/10/92	4	0.24	L6	2.39	20.2	BO		
12/9/88	7/5/93	24	1.44	EN3	4.65	1.73	BO		
19/10/88	7/6/93	23	1.38	EN3	4.63	1.82	BO		
16/11/88	7/6/93	23	1.38	EN3	4.56	1.85	BO		
14/11/88	23/9/93	23	1.38	EN3	4.77	1.76	BO		
18/11/88	30/11/93	23	1.38	EN3	5.03	1.67	BO		
6/12/88	15/2/94	23	1.38	EN3	5.19	1.62	BO	21.7	33.5
25/10/88	15/4/94	23	1.38	EN3	5.47	1.54	BO	19.0	29.4
25/10/88	14/6/94	23	1.38	EN3	5.64	1.49	BO	16.9	26.0
12/4/89	9/7/94	24	1.44	EN3	4.24	1.90	BO	15.5	24.0

Table 3. Summary of the results obtained with the CR39 subdetector of MACRO. At present 18.37 m^2 of CR39 have been analysed.

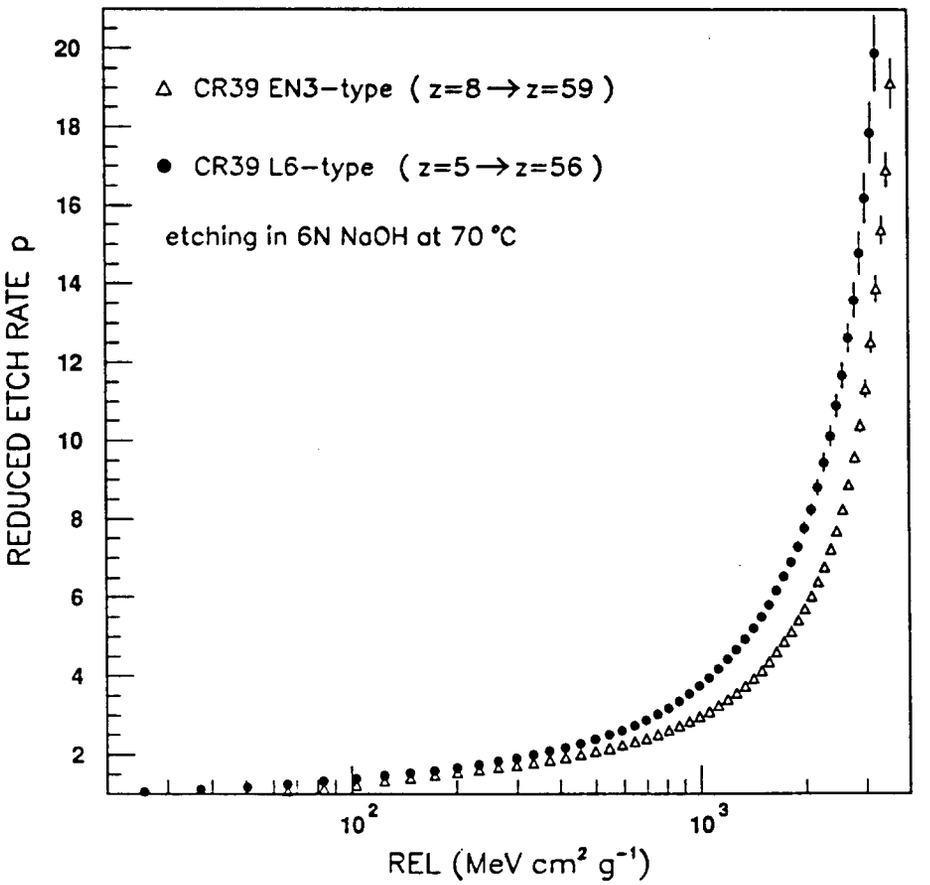
△ CR39 EN3–type (z=8 → z=59)
● CR39 L6–type (z=5 → z=56)
etching in 6N NaOH at 70 °C
REDUCED ETCH RATE ρ
REL (MeV cm² g⁻¹)
20
18
16
14
12
10
8
6
4
2
10²
10³

Fig. 1

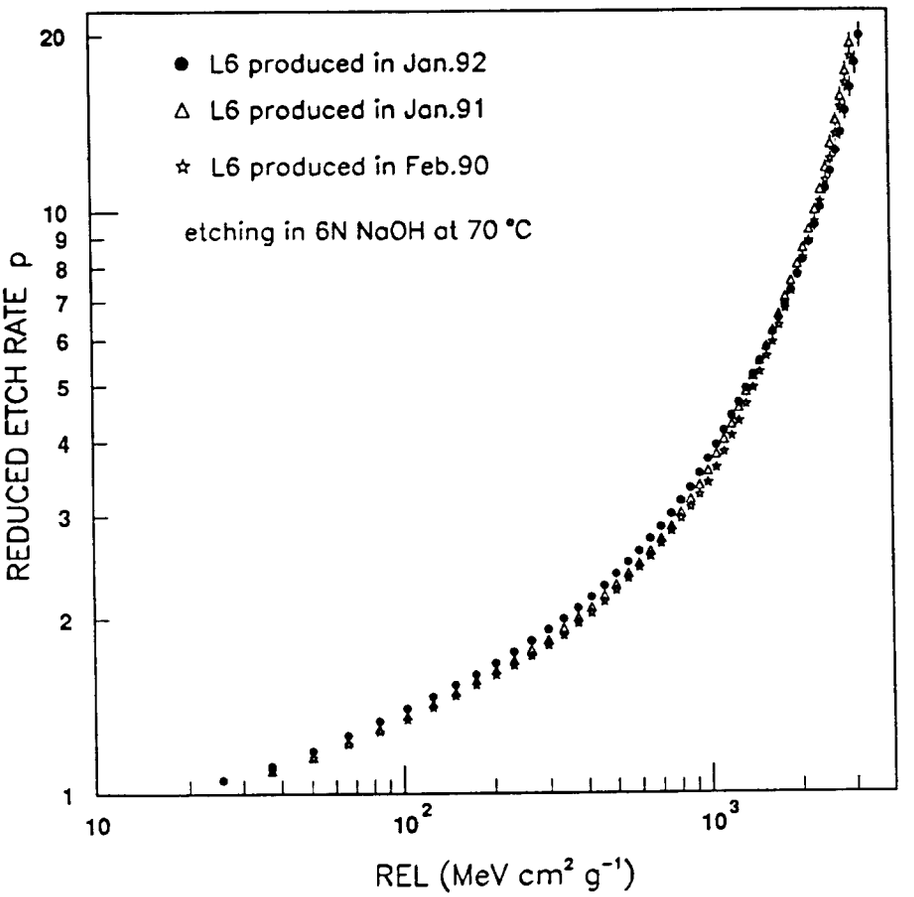
● L6 produced in Jan.92
△ L6 produced in Jan.91
☆ L6 produced in Feb.90
etching in 6N NaOH at 70 °C
REDUCED ETCH RATE p
REL (MeV cm² g⁻¹)
20
10
9
8
7
6
5
4
3
2
1
10
10²
10³

Fig.2

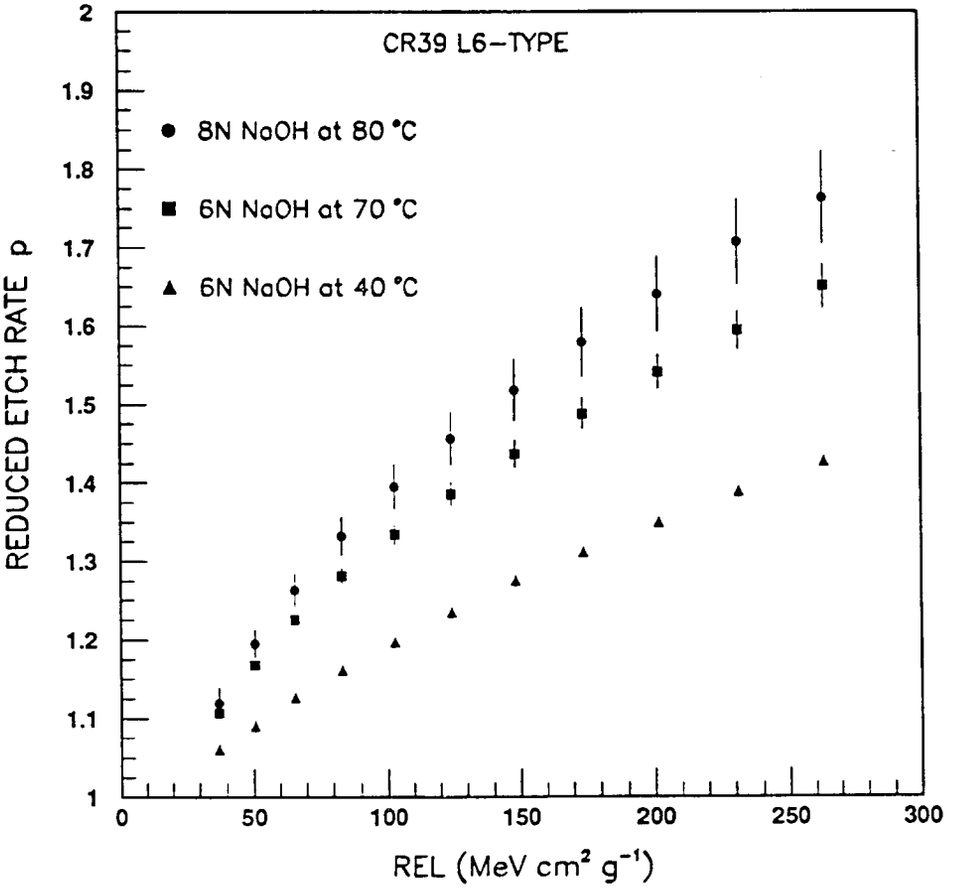
CR39 L6–TYPE
8N NaOH at 80 °C
6N NaOH at 70 °C
6N NaOH at 40 °C
REDUCED ETCH RATE p
REL (MeV cm² g⁻¹)
2
1.9
1.8
1.7
1.6
1.5
1.4
1.3
1.2
1.1
1
0
50
100
150
200
250
300

Fig.3

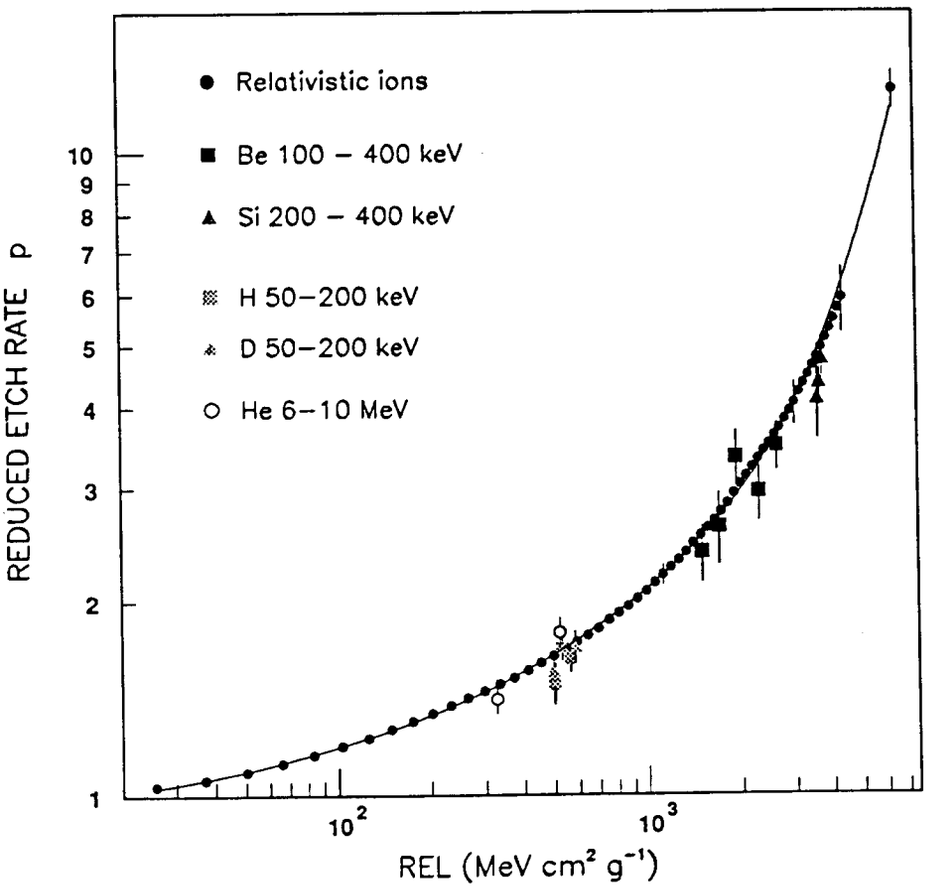
Relativistic ions
Be 100 – 400 keV
Si 200 – 400 keV
H 50–200 keV
D 50–200 keV
He 6–10 MeV
REDUCED ETCH RATE p
10
9
8
7
6
5
4
3
2
1
10^2
10^3
REL (MeV cm^2 g^{-1})

Fig.4

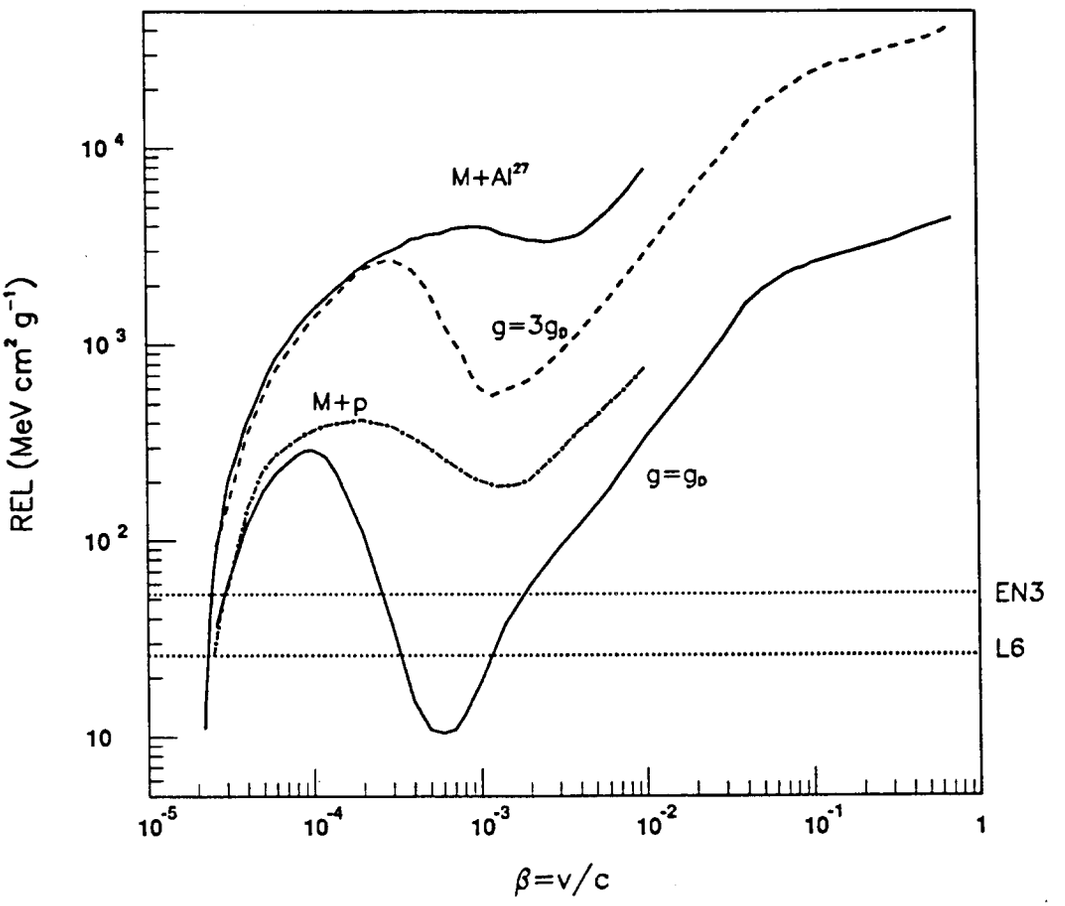
REL (MeV cm² g⁻¹)
10⁴
10³
10²
10
M+Al²⁷
g=3g₀
M+p
g=g₀
EN3
L6
10⁻⁵
10⁻⁴
10⁻³
10⁻²
10⁻¹
1
β=v/c

Fig. 5

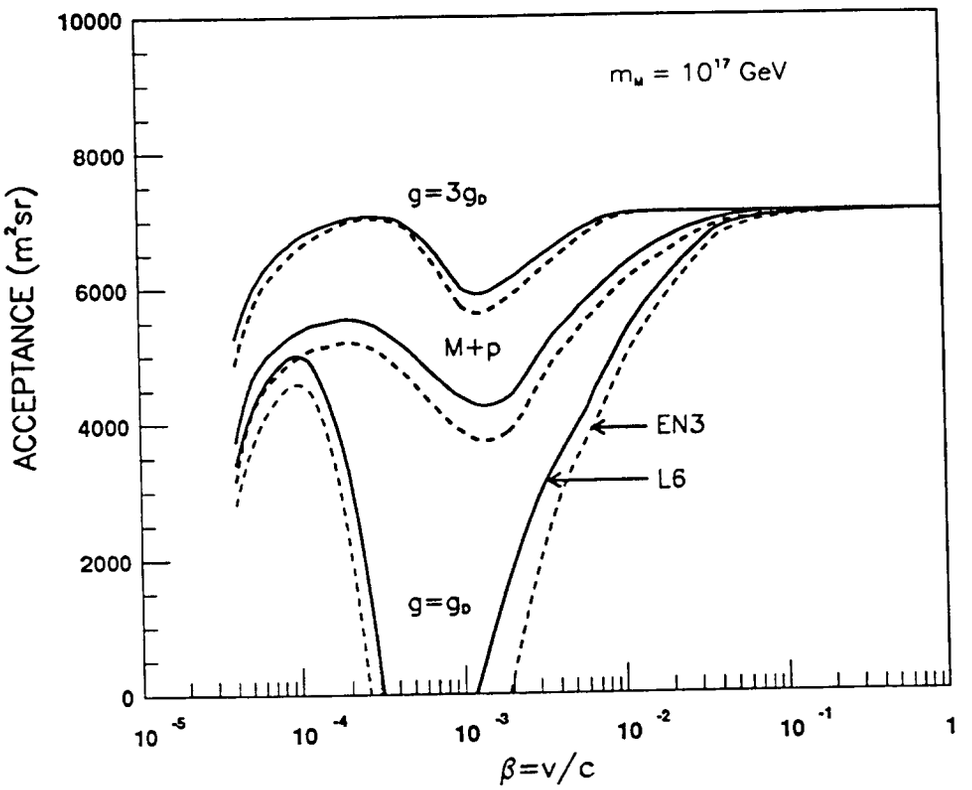
10000
8000
6000
4000
2000
0
ACCEPTANCE (m²sr)
m_M = 10^17 GeV
g=3g_D
M+p
EN3
L6
g=g_D
10^-5
10^-4
10^-3
10^-2
10^-1
1
β=v/c

Fig. 6

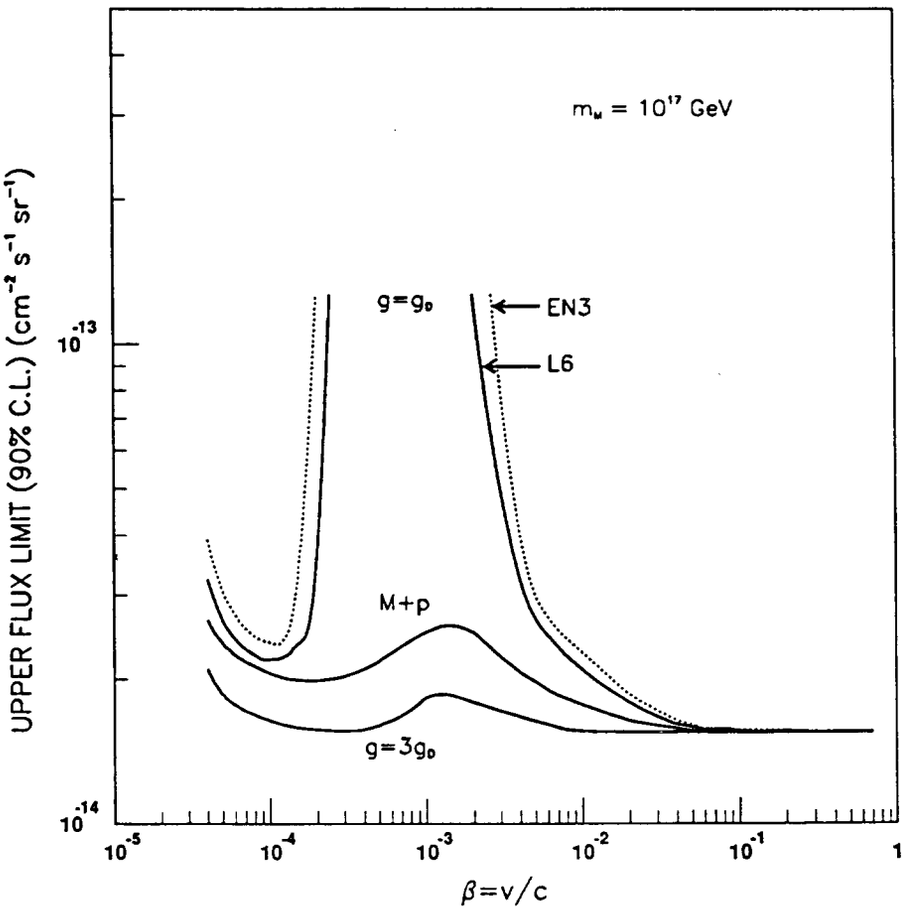
m_M = 10^{17} GeV
g=g$_0$
EN3
L6
M+p
g=3g$_0$
UPPER FLUX LIMIT (90% C.L.) (cm^{-2} s^{-1} sr^{-1})
10^{-13}
10^{-14}
10^{-5}
10^{-4}
10^{-3}
10^{-2}
10^{-1}
1
β=v/c

Fig. 7